available at www.sciencedirect.com

SCIENCE DIRECT®

journal homepage: www.elsevier.com/locate/biochempharm

Sensitization of breast carcinoma cells to ionizing radiation by small molecule inhibitors of DNA-dependent protein kinase and ataxia telangiectsia mutated

Ian G. Cowell *, *Barbara W. Durkacz*, *Michael J. Tilby*

Northern Institute for Cancer Research, Paul O'Gorman Building, Medical School, University of Newcastle, Newcastle upon Tyne, NE2 4HH, UK

ARTICLE INFO

Article history:
Received 15 August 2005
Accepted 29 September 2005

Keywords:
ATM
DNA-PK
DNA repair
Histone H2AX
Radiosensitivity
Breast cancer

Abbreviations:
A-T, ataxia telangiectasia
DNA-PK, DNA-dependent protein kinase
DNA-PKcs, DNA-PK catalytic subunit
ATM, ataxia telangiectasia mutated
ATR, ataxia telangiectasia and Rad3 related
ATRIP, ATR-interacting protein
RPA, replication protein A
NHEJ, non-homologous end joining
DSB, DNA double-strand break
PIKK, phosphatidylinositol 3′-kinase like kinase
IR, ionising radiation
HRR, homologous recombination repair

ABSTRACT

DNA-PK and ATM are members of the phosphatidylinositol 3′-kinase like kinase (PIKK) family of serine/threonine protein kinases and have critical roles in the cellular response to DNA double-strand breaks. Genetic loss of either activity leads to pronounced sensitivity to ionizing radiation (IR). Hence, these enzymes are potential targets to confer enhanced radiosensitivity on tumour cells. We show that novel inhibitors of either DNA-PK or ATM sensitize breast carcinoma cells to IR. Radiosensitization was accompanied by an apparent DNA repair deficit as measured by the persistence of IR-induced foci of phosphorylated histone H2AX (γH2AX foci). These specific inhibitors also allowed us to probe the biochemistry and kinetics of histone H2AX phosphorylation following γ-irradiation in breast cancer cells with the aim of validating H2AX as a biomarker for DNA-PK or ATM inhibition in vivo. ATM inhibition reduced the initial average intensity of γH2AX foci while inhibition of DNA-PK had only a small effect on the initial phosphorylation of H2AX. However, simultaneous treatment with both compounds dramatically reduced γH2AX focus intensity, consistent with the reported role of ATM and DNA-PK in IR induced phosphorylation of H2AX.

* *Corresponding author*. Tel.: +44 191 246 4352; fax: +44 191 246 4301.
E-mail address: i.g.cowell@ncl.ac.uk (I.G. Cowell).
0006-2952/$ – see front matter
doi:10.1016/j.bcp.2005.09.029

1. Introduction

Radiotherapy remains a central component of current treatments for cancer. In early breast cancer for example, it is used as an adjunct to surgery in the majority of cases [1]. The effectiveness of radiotherapy is limited by the recovery of tumour versus normal tissues, and many tumours are refractory to radiotherapy alone. One strategy to improve the effectiveness of radiotherapy is modulation of tumour radiosensitivity. The cytotoxicity of IR is mainly mediated through the generation of DNA-double strand breaks (DSBs) as evidenced by the pronounced radiosensitivity of cells and organisms defective in the machinery of DSB repair [2]. Thus, pharmacological inhibition of DSB repair provides a mechanism to potentiate the cytotoxicity of IR in tumour cells.

The majority of IR-induced DSBs are repaired by non-homologous end joining (NHEJ) in vertebrate cells, with some contribution from homologous recombination-mediated repair (HRR) [3,4]. Efficient NHEJ requires the DNA ligase IV/Xrcc4/Artemis complex and DNA-dependent protein kinase (DNA-PK). The DNA-PK catalytic subunit (DNA-PKcs) is a member of the phosphatidylinositol 3-kinase like kinase (PIKK) family of serine/threonine protein kinases which also includes ataxia telangiectasia mutated (ATM), ataxia telangiectasia and Rad3 related (ATR), hSMG1 and mTOR. ATM is a key regulator of the cellular response to DSBs [5]. It is rapidly activated following IR, whereupon it phosphorylates proteins involved in cell cycle checkpoints and DNA repair. In addition, ATM modulates NF-κB activity and phosphorylates histone H2AX and a number of other factors that accumulate at DSBs [5]. Cells lacking ATM are radiosensitive, display defective cell cycle arrest following DNA damage, and exhibit DNA repair deficits [6]. Recent reports describe a requirement for ATM in the repair of a subset of DSBs by NHEJ [7,8]. In addition, evidence exists that ATM has a role in modulating HRR [9,10].

Thus, DNA-PK and ATM represent attractive candidates for pharmacological inhibition to achieve therapeutically valuable radiosensitization. A number of compounds have been described as inhibitors of PIKKs, with varying specificities for DNA-PK, ATM or other kinases. While recently developed inhibitors such as NU7441 and KU-55933 are highly specific for DNA-PK or ATM, respectively [11–13], older compounds such as wortmannin and LY294002 lack specificity [14–17] making them unsuitable for clinical use.

The aims of the work presented here were firstly to confirm that the specific DNA-PK inhibitor NU7441 and the specific ATM inhibitor KU-55933 radiosensitized a breast cancer cell line by the mechanisms predicted and to determine if their effects were additive. Secondly, we aimed to define the effects of these inhibitors on the formation and persistence of foci of phosphorylated histone H2AX in order to establish the feasibility of using these as a biomarker of pharmacodynamic effects of these compounds in clinical trials.

2. Materials and methods

2.1. Inhibitors

8-Dibenzothiophen-4-yl-2-morpholin-4-yl-chromen-4-one (NU7441) and 2-morpholin-4-yl-6-thianthren-1-yl-pyran-4-one (KU-55933) were dissolved in DMSO and stored at −20 °C. Inhibitors were added to cell cultures such that the final DMSO concentrations were kept constant at 0.25% (v/v). NU7441 was obtained from Prof. Roger Griffin and was synthesised at the Northern Institute for Cancer Research, University of Newcastle (Newcastle upon Tyne, United Kingdom) in collaboration with KuDOS Pharmaceuticals (Cambridge, United Kingdom). KU-55933 was obtained from Dr. Graeme Smith, KuDOS Pharmaceuticals (Cambridge, United Kingdom).

2.2. Cell lines and culture

MCF7 cells were cultured as monolayers in RPMI 1640 medium supplemented with 10% (v/v) FCS, 100 units/mL penicillin.

2.3. Western blotting

For whole cell extracts, cells at approximately 70% confluence were scraped from dishes into ice cold PBS, pelleted and resuspended in four packed cell volumes of lysis buffer [0.25% SDS (w/v), 10 mM $MgCl_2$, 50 mM Tris–HCl, pH 7.4, 50 μg/mL DNase I, protease inhibitors, phosphatase inhibitors]. After incubation on ice for 30 min two volumes of solubilization buffer [2% SDS, 20% glycerol, 5% β-mercaptoethanol, 0.6 M Tris–HCl, pH 7.2] were added and the lysates were incubated at 70 °C for 10 min. Samples were stored at −20 °C before protein estimation and electrophoresis. SDS PAGE was performed using 4–20% Tris–glycine gradient gels. These were transferred by standard methods to nitrocellulose. Antibody binding was detected by chemiluminescence. Antibodies used were rabbit polyclonal anti-γH2AX (Upstate), rabbit anti-H2A.X (Abcam), rabbit anti-$p53_{Ser15P}$ (ab1431, Abcam), mouse anti-$ATM_{Ser1981\text{-}P}$ (10H11.E12, Upstate) and mouse anti-ATM (5C2, Abcam). Blots previously probed with anti-$H2AX_{Ser139\text{-}P}$ or anti-$ATM_{Ser1981\text{-}P}$ were stripped and reprobed with antibodies directed to non phospho-specific H2AX and ATM as loading controls.

2.4. Immunofluorescence

MCF7 cells were grown on glass coverslips to 50–70% confluence. Following X-irradiation (2.9 Gy/min at 230 kV, 10 mA) cells were returned to the incubator for the described length of time before fixation. Coverslips were washed in PBS and fixed in methanol at −20 °C for 5 min before washing three times for 10 min each in PBS. Blocking was carried out for 1–18 h in KCM [120 mM KCl, 20 mM NaCl, 10 mM Tris–HCl, pH 7.5, 0.5 mM EDTA, 0.1% (v/v) Triton X-100] containing 10% (w/v) dried milk powder and 2% (w/v) BSA. Antibody incubation was carried out in the same solution and washes were performed using KCM. Antibodies used were mouse monoclonal anti-γH2AX (Upstate) and Alexa Fluor® 546 goat anti-mouse IgG (Molecular Probes). Cells were counterstained with DAPI before mounting. Images were obtained using Olympus

BH2-RFCA fluorescence microscope fitted with a xenon lamp and a 40X objective (DplanApo 40UV). Separate 16-bit grey-scale images were recorded for DAPI and Alexa 546 using a Hamamatu ORCA$_{II}$ BT-1024 cooled CCD camera. Image Pro Plus software (Media Cybernetics) was used for image capture and quantitative image analysis. Subsequent image handling was carried out in Photoshop.

2.5. *Cell death assessment*

MCF7 cells were grown on glass coverslips. Following X-irradiation (2.9 Gy/min at 230 kV, 10 mA) cells were returned to the incubator for 24 or 48 h before staining unfixed cells with propidium iodide and Annexin-V-fluorescein (Annexin-V-Fluos kit, Roche Basel, Switzerland). Images were collected by phase contrast and fluorescent microscopy from three coverslips per treatment.

2.6. *Cytotoxicity assays*

Exponentially growing MCF7 cells were exposed to inhibitors for 1 h prior to γ-irradiation (3.1 Gy/min). Cells were incubated for 18 h at 37 °C in the presence of inhibitor(s) before trypsinising, counting and reseeding for colony formation in the absence of inhibitors. Data were normalized to untreated controls exposed to solvent alone (0.25% DMSO).

3. Results

3.1. *Inhibition of ATM in intact cells*

NU7441 and KU-55933 (Fig. 1A) have IC$_{50}$ values for DNA-PKcs and ATM of 14 nM and 13 nM, respectively in vitro and are specific in respect to other PIKKs [13,18]. To assess the ability of KU-55933 to inhibit ATM in breast cancer cells we examined several downstream targets of ATM by Western blot analysis of whole cell extracts from irradiated MCF7 cells. DSBs activate ATM through a process leading to autophosphorylation on serine 1981 [19]. ATM$_{Ser1981}$ phosphorylation was rapidly induced upon irradiation of MCF7 cells and this induction was fully inhibited by KU-55933 (Fig. 1B). Similarly, KU-55933 inhibited IR-induced phosphorylation of p53 on serine 15 (Fig. 1C), a process that has been shown to be ATM-dependent [20]. KU-55933 also inhibited the phosphorylation of histone H2AX serine 139 (Fig. 1B and C), a process that is partially dependent upon ATM [21,22]. By contrast, NU7441 exhibited little or no inhibition of IR-induced ATM$_{Ser-1981}$ phosphorylation and had little effect on H2AX$_{ser139}$ phosphorylation 60 min after irradiation (Fig. 1B). By analyzing the levels of H2AX phosphorylation and p53 phosphorylation it was possible to determine the lowest concentration of KU-55933 to maximally inhibit cellular ATM function. Phospho-ser15 p53 was readily detectable in extracts prepared 30 min after γ-irradiation in the absence of inhibitor but was reduced to an undetectable level by preincubation with 2 μM KU-55933. Similarly, phosphorylation of H2AX was maximally inhibited by 5 μM KU-55933 (Fig. 1C).

3.2. *NU7441 and KU-55933 radiosensitize MCF7 breast carcinoma cells*

The effects of NU7441 and KU-55933 on the sensitivity of MCF7 cells to γ-radiation were examined both singly and in combination using clonogenic survival assays. Initially, cells were exposed to 0 or 2 Gy in the presence of increasing concentrations of either NU7441 or KU-55933 before plating for colony formation. In the absence of IR the inhibitors had no significant effect on clonogenic cell survival at concentrations up to 2 μM for NU7441 and 20 μM for KU-55933 or in combination at 1 and 10 μM, respectively (Fig. 2A and B). Additionally, no significant growth inhibition was detected in MCF7 cells under continuous exposure to NU7441 or KU-55933 at concentrations up to 1 or 10 μM, respectively, using a colorimetric growth inhibition assay (data not shown). However, when cells were irradiated in the presence of increasing concentrations of NU7441 or KU-55933, substantial potentiation of IR-induced killing was observed. Mean clonogenic survival after 2 Gy was reduced 40 fold by 1 μM NU7441 and only fell marginally when the concentration was

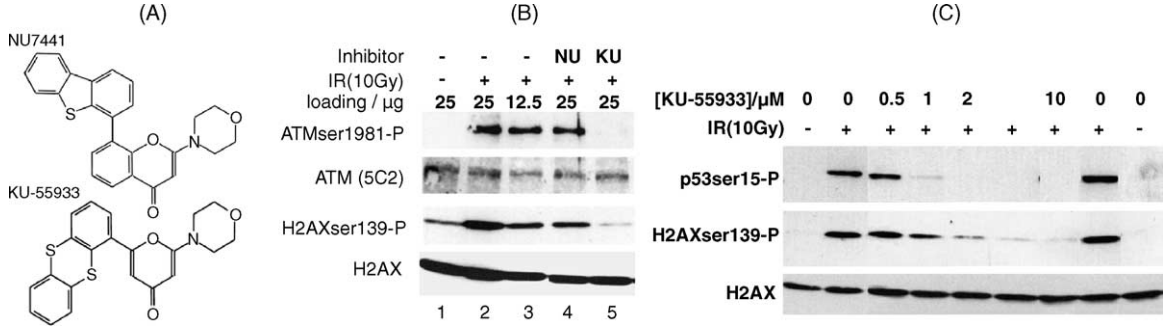

Fig. 1 – (A) Chemical structures of NU7441 and KU-55933. (B) KU-55933 but not NU7441 inhibits ATM kinase activity in vivo. MCF7 cells were preincubated in medium containing 1 μM NU7441 (NU), 10 μM KU-55933 (KU) or solvent alone (–) for 1 h prior to mock irradiation or γ-irradiation (10 Gy). 60 min after irradiation, cell extracts were prepared and analysed by western blot analysis using the antibodies shown. (C) Dose response for ATM inhibition by KU-55933. MCF7 cells were incubated in medium containing various concentrations of KU-55933 for 1 h prior to X-irradiation (10 Gy at 7.1 Gy/min) or mock irradiation as indicated. Cell extracts were prepared 30 min after irradiation and these were analysed for p53 phospho-serine 15 and H2AX phosphor-serine 139 by western blotting.

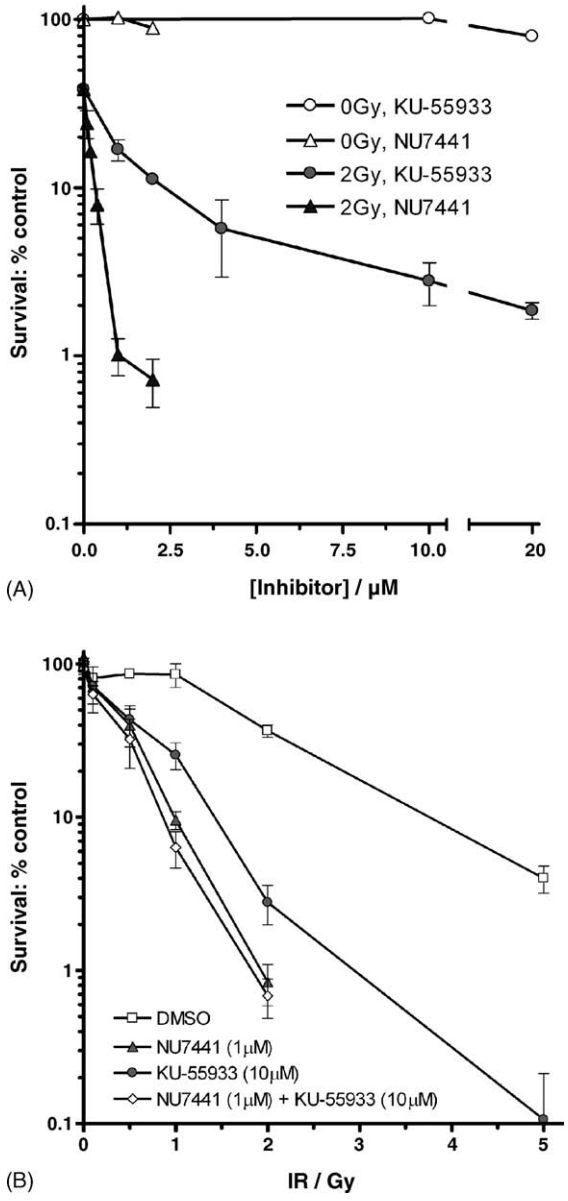

Fig. 2 – NU7441 and KU-55933 sensitize MCF7 breast carcinoma cells to ionizing radiation. (A) MCF7 cells were incubated in medium containing varying concentrations of KU-55933 or NU7441 for 1 h prior to γ-irradiation or mock irradiation. Cells were allowed to recover for 18 h in the presence of inhibitor before trypsinization, counting and plating for colony formation. Non-irradiated cells + KU-55933 (○); non-irradiated cells + NU7441 (△), γ-irradiated cells + KU55933 (●); γ-irradiated cells + NU7441 (▲). (B) MCF7 cells were incubated in medium containing solvent alone (□), 10 μM KU-55933 (●), 1 μM NU7441 (▲), or both inhibitors (◇) for 1 h prior to γ-irradiation at doses between 0 and 5 Gy. Data are the mean of at least three independent experiments ± S.E.

doubled (Fig. 2A). Thus, NU7441 was used at 1 μM in subsequent experiments. For KU-55933, clonogenic survival was reduced 13-fold at a concentration of 10 μM and only fell marginally when the concentration of inhibitor was raised to 20 μM (Fig. 2A). Thus, KU-55933 was used at 10 μM for subsequent experiments. Next, clonogenic survival assays were carried out where MCF7 cells were exposed to a range of γ-radiation doses in the presence of fixed concentrations of NU7441, KU-55933, a combination of both inhibitors or vehicle alone (Fig. 2B). The inhibitors significantly enhanced the cytotoxic effect of IR, even at doses as low as 0.5 Gy. The effects of NU7441 and KU-55933 on the survival of cells exposed to 1–2 Gy are summarized in Table 1. PF_{90} values were highly significant ($P < 0.0005$, *t*-test) for each inhibitor and in combination. Notably, NU7441 produced a greater effect ($P < 0.05$) than KU-5993. The potentiation associated with the use of both inhibitors in combination was not significantly different to the value obtained with NU7441 alone ($P = 0.35$), leading to the conclusion that under these conditions, the two inhibitors do not act synergistically and have little if any additive effect.

Table 1 – Radiosensitization of MCF7 cells by NU7441 and KU-55933

Inhibitor	Survival ratio[a]		PF_{90}[b]
	1 Gy	2 Gy	
NU7441 (1 μM)	10.6 ± 2.5	51.9 ± 11.2	4.0 ± 0.14
KU-55933 (10 μM)	4.1 ± 0.56	15.9 ± 3.4	2.8 ± 0.29
Combination	16.2 ± 5.3	70 ± 21	5.2 ± 1.14

[a] Survival ratios were calculated by dividing clonogenic survival in the presence of vehicle alone by that in the presence of inhibitor. Mean ratios and standard errors were determined from three independent experiments.

[b] PF_{90} is the ratio of the LD_{90} (radiation dose resulting in 10% survival) values obtained in the presence of vehicle alone divided by those obtained in the presence of inhibitor.

3.3. *Effects of NU7441 and KU-55933 on γH2AX focus dynamics*

γH2AX foci are a well-characterised indicator of the early cellular response to IR and have been suggested as surrogates for DNA DSBs [23–26]. We observed the effects of each inhibitor on γH2AX focus dynamics in MCF7 cells (see Fig. 3A). As reported by others [23], a small number of bright γH2AX foci were observed in non-irradiated MCF7 cells (mean = 3.0). These foci were not affected in number or intensity by prior incubation (2 h) of the cells with either inhibitor. In the presence of carrier alone, bright foci were apparent in all cells 15 min after X-irradiation (2 Gy). The number of γH2AX foci subsequently declined to near background levels by 22 h (Fig. 3A and B). The DNA-PK inhibitor NU7441 (1 μM) did not significantly affect the number or brightness of foci visible 15 min after irradiation, but the subsequent decline in focus numbers over the period of the experiment (22 h) was much smaller than for the control cells. For cells irradiated in the presence of NU7441, the mean number of γH2AX foci per cell 22 h after irradiation remained at 54% of the number present at 15 min, but for cells irradiated in the absence of inhibitor, the figure was 16%. When cells were irradiated in the presence of KU-55933, the initial nuclear γH2AX fluorescent intensity was lower than for control cells (Fig. 3A and C). Despite the reduced intensity, foci were clearly apparent 15 min post-

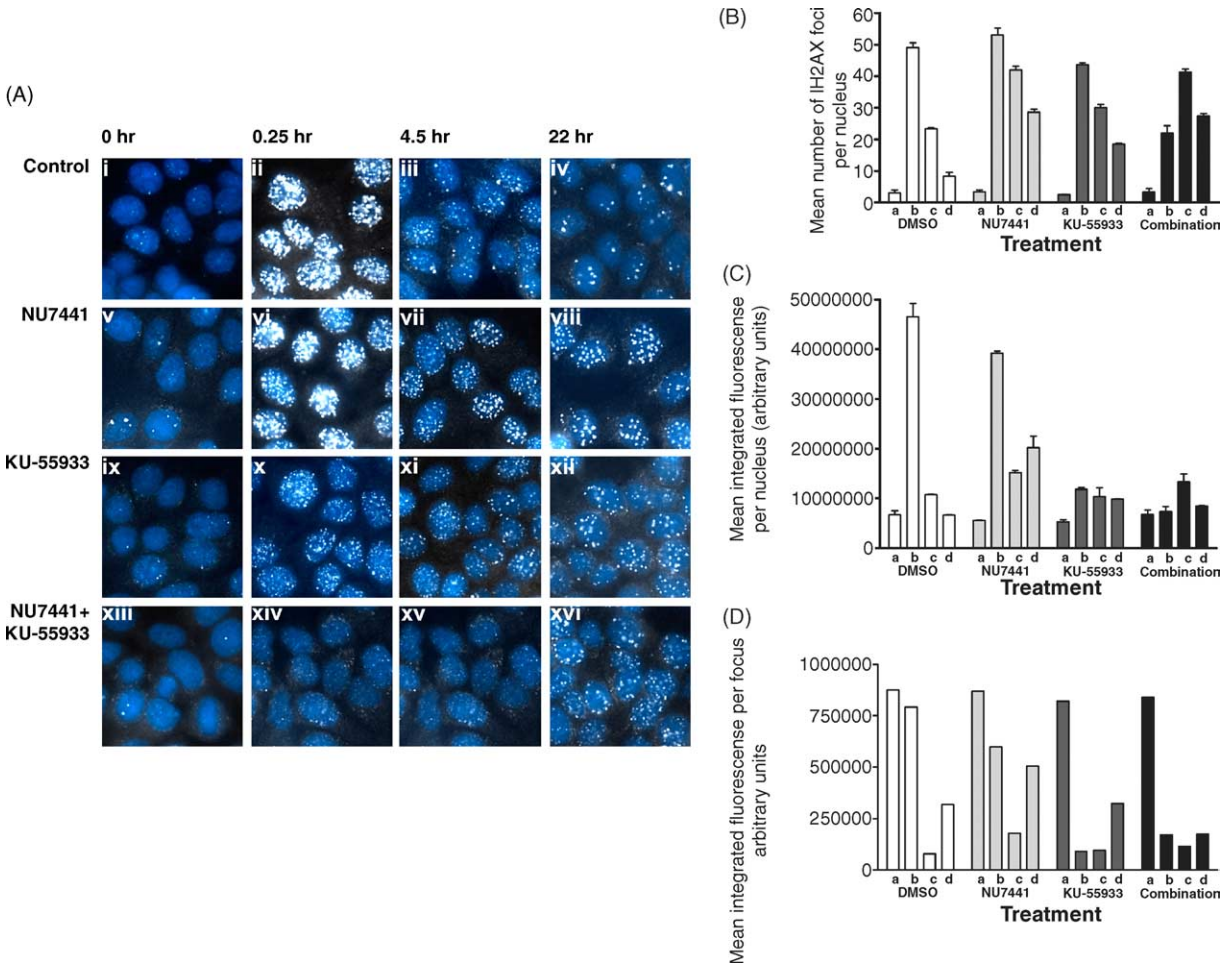

Fig. 3 – Effects of NU7441 and KU-55933 on IR-induced γH2AX focus formation and decay. (A) MCF7 cells grown on coverslips were incubated in medium containing 1 μM NU7441, 10 μM KU-55933, 1 μM NU7441 plus 10 μM KU-55933 or solvent alone (Control, DMSO) for 1 h prior to X-irradiation (2 Gy). Cells were fixed at the times indicated and processed for γH2AX immunofluorescence. Zero hour represents non-irradiated cells. Sixteen bit greyscale images were recorded and DAPI (blue) and γH2AX (white) images were superimposed. Representative areas from one image for each treatment are shown. (B) Mean number of γH2AX foci per cell ± S.E.M. for each inhibitor treatment in a, non-irradiated cells; b, 15 min after 2 Gy; c, 4.5 h after 2 Gy and d, 22 h after 2 Gy. (C) Mean integrated fluorescence values. The total fluorescence signal emanating from each nucleus in at least two images per treatment was determined as described in Section 2. The means of these integrated fluorescence values are plotted together with S.E. values. (D) Time course of appearance and loss of focal γH2AX after exposure to IR. Nuclear integrated fluorescence values were corrected for background (interfocal) fluorescence and mean corrected integrated fluorescence values were divided by the mean number of foci per nucleus for each treatment and time point to derive a value for the mean integrated fluorescence per focus (a, non-irradiated cells, b, 15 min after 2 Gy; c, 4.5 h after 2 Gy and d, 22 h after 2 Gy).

irradiation (Fig. 3A). The number of foci scored for KU55933-treated cells was slightly lower (11%) than for control cells at 15 min, presumably due to the reduced fluorescence intensity. As with NU7441, focus numbers declined more slowly in the presence of KU-55933 than in control (DMSO treated) cells, with 45% of the number present at 15 min still visible by 22 h. Focal fluorescence intensity appeared to increase between 15 min and 22 h in KU-55933 treated cells (Fig. 3A, panels ix–xii), and this was borne out by integrated nuclear fluorescence measurements (Fig. 3C). The average nuclear fluorescence fell only slightly between 15 min and 22 h while the number of foci more than halved. This can be seen more clearly in Fig. 3D, where average integrated nuclear fluorescence values corrected for background inter-focal fluorescence, are divided by the mean number of foci. The appearance of γH2AX foci was considerably delayed in cells irradiated in the presence of both inhibitors (Fig. 3A–C).

3.4. *Average γH2AX focus intensity is not constant with time after exposure to ionising radiation*

The average intensity of γH2AX foci formed in the presence of vehicle alone or NU7441 decreased between 15 min and 4.5 h. However, 22 h after irradiation, bright γH2AX foci were again present with average focus intensity close to the brightness observed at 15 min. This was apparent by visual inspection of

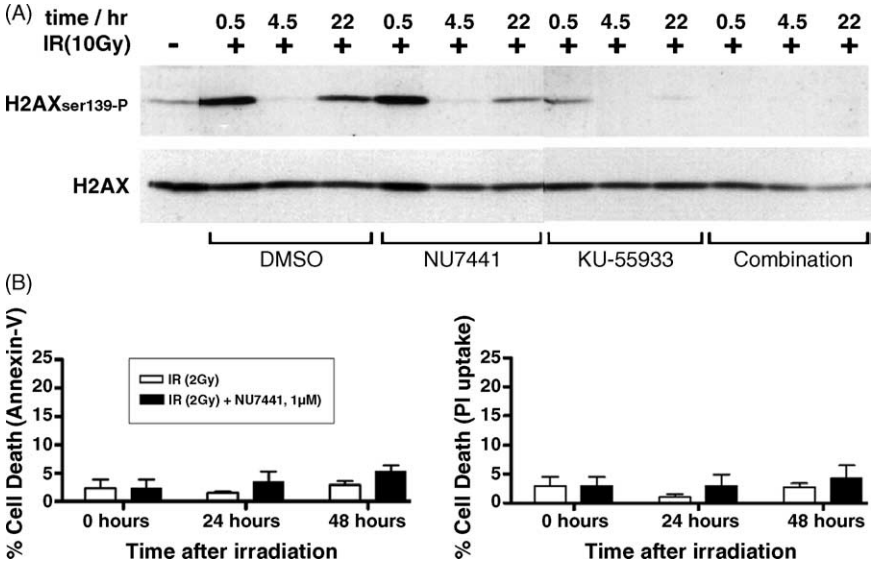

Fig. 4 – (A) Cells were incubated in medium containing solvent (DMSO), NU7441 (1 μM), KU-55933 (10 μM) or both NU7441 and KU-55933 for 1 h prior to X-irradiation (10 Gy at 7.1 Gy/min) or mock irradiation as indicated. Whole cell extracts were prepared after 30 min, 4.5 h or 22 h and these were analysed for H2AX phosphor-serine 139 by western blotting. The blot was subsequently stripped and re-probed for bulk H2AX. (B) Abundance of apoptotic cells in non-irradiated cells (0 h) and irradiated cells (24 and 48 h). Uptake of propidium iodide and Annexin-V staining was determined for cells grown on coverslips by fluorescent microscopy.

the images (Fig. 3A), by observing the mean fluorescence intensity per focus (Fig. 3D) and by directly measuring the distribution of fluorescence values from foci found in representative cells at each time point (data not shown). This unexpected pattern of H2AX phosphorylation was confirmed by Western blotting (Fig. 4A). A strong γH2AX signal was detected as expected 15 min after irradiation but by 4.5 h the signal was dramatically reduced. However, a clear γH2AX signal was again detected in extracts collected 24 h after irradiation. This was true for cells irradiated in the absence of inhibitor and for cells irradiated in the presence of NU7441. Notably, the proportion of cells displaying apoptotic properties (Annexin-V staining or propidium iodide uptake) remained low (<4%) up to 48 h after MCF7 cells were exposed to 2 Gy IR in a parallel experiement (Fig. 4B).

4. Discussion

DNA-PK deficient and A-T cells are characterised by pronounced radiosensitivity and this has stimulated the search for DNA-PK and ATM inhibitors that potentiate the anti-tumour effects of ionizing radiation and agents such as topoisomerase II poisons. We have shown pronounced radiosensitization of MCF7 breast carcinoma cells following inhibition of either DNA-PKcs (by NU7441) or ATM (by KU-55933). Cell survival in a clonogenic assay following a 2 Gy γ-radiation dose was significantly reduced by NU7441 and KU-55933 (Fig. 2, Table 1). The dose of radiation required to reduce cell survival to 10% of the control was reduced from 3.8 to 1.4 Gy by KU-55933 and to 0.95 Gy by NU7441. Notably, inhibition of DNA-PK by NU7441 resulted in a greater degree of radiosensitization than did treatment with KU-55933 and no significant additive effect was observed when the compounds were combined (Fig. 2B). This is perhaps surprising as while inhibition of DNA-PK would be expected to seriously compromise NHEJ, evidence from chicken DT40 cells suggests that loss of ATM would affect HR-mediated repair [10]. Thus, combined use of both drugs, by inhibiting two independent repair pathways, was anticipated to produce a larger repair deficit and a corresponding greater radiosensitization than either compound alone. However, DT40 cells are extremely proficient in HR and the relative contribution of HR-mediated repair in these cells is probably considerably greater than in cells such as MCF7 cells. In addition, recent evidence supports a role for ATM in a subset of NHEJ events [7,8]. Notably, Riballo et al. [8] showed that while inhibition of ATM reduced DNA repair in wild-type fibroblasts, it did not further affect DNA repair in NHEJ defective cells (lig4$^{-/-}$). Thus, it is likely that the molecular events underlying the radiosensitizing capacity of NU7441 and KU-5993 lie predominantly in the same pathway (NHEJ). Furthermore, autophosphorylation of DNA-PK is thought to be necessary for events after recruitment of DNA-PKcs to DSBs and for its ultimate dissociation [27]. Therefore, catalytically inhibited DNA-PK may block access to other repair factors and other repair pathways. This explanation has also been suggested by Allen et al. [28] to account for the inhibition of radiation induced HR by the DNA-PK inhibitor IC86621 in DNA-PK wt but not DNA-PK deficient cells and is further supported by the finding that DNA-PK deficient hamster V3 cells engineered to express an autophosphorylation deficient DNA-PKcs mutant are more radiosensitive than the parent V3 cell line [29].

Analysis of γH2AX foci provides a useful surrogate for DSB formation and subsequent repair following clinically relevant doses of radiation [24–26]. We have shown that both inhibitors

lead to a persistence of γH2AX foci after exposure to IR. Inhibition of DNA-PK and ATM in MCF7 cells produced quantitatively very similar results with regards to γH2AX focus dynamics to those comparing wild type, LIG4$^{-/-}$ and A-T fibroblasts reported by Khune et al. [7] which in turn closely mimicked repair kinetics measured by PFGE after higher radiation doses. This strongly supports the contention that NU7441 and KU-55933 radiosensitize cells through an induced DNA repair deficit recapitulating genetic loss of NHEJ core components or ATM, respectively.

Notwithstanding an early report that IR-induced phosphorylation of H2AX is dependent upon ATM [30] the weight of evidence now supports an at least partially redundant role for ATM and DNA-PK [21,22]. ATR may also contribute to IR-induced phosphorylation of ATM substrates such as H2AX at later times in cells lacking ATM activity [5] and ATR is implicated in H2AX phosphorylation as a result of replication stress [31]. Our results are consistent with this, but suggest that ATM is the major phosphorylator of H2AX in MCF7 cells shortly after exposure to ionizing radiation. NU7441 had a small effect on the H2AX fluorescence intensity 15 min after irradiation (the shortest time used), but KU-55933 reduced the intensity approximately eight-fold (Fig. 3C and D). Combined use of both inhibitors substantially inhibited H2AX phosphorylation, but nonetheless, reasonably bright foci had formed by 22 h (Fig. 3A, panel xvi). This apparently DNA-PK and ATM independent phosphorylation of H2AX may be due a low level of residual enzyme activity. Alternatively it could have resulted from the activation of ATR, either as cells pass through S-phase, or possibly by recruitment of ATR/ATRP RPA binding to ssDNA formed at remaining DSBs, as demonstrated by Zhou and Elledge [32]. We noticed a transient fall in the fluorescent signal per focus in the absence of inhibitor or in the presence of NU7441. As shown in Fig. 3D, the fluorescence intensity of γH2AX foci measured at 4.5 h post-irradiation was substantially lower than at 15 min or 22 h and this was mirrored by Western blotting data (Fig. 4A). The reduction in average γH2AX focus intensity reported here at 4.5 h compared to 15 min may be explained by the ongoing dephosphorylation or exchange of γH2AX molecules at chromatin sites where repair has occurred. The appearance of brighter foci at later times in most cells cannot be explained by chromatin cleavage and H2AX phosphorylation associated with apoptosis, as the proportion of cells exhibiting apoptotic features (Annexin V or propidium iodide staining) remained below 4% 24 h after irradiation (Fig. 4B) In addition, transit through S-phase was not required as the same pattern of focus intensity occurred in serum-starved non-proliferating cells (see Supplementary material). It is possible that the bright foci observed in control and NU7441 treated cells 22 h after irradiation and the eventual appearance of foci in cells treated with both inhibitors could be due to the appearance of ssDNA at unrepaired DSBs and recruitment of ATR resulting in increased phosphorylation of H2AX. This possibility is currently under investigation.

In conclusion, we report the radiosensitization of a breast cancer cell line using specific inhibitors of DNA-PK and ATM. The increased sensitivity to ionizing radiation was associated with reduced clearance of γH2AX foci. This supports the view that inhibitors of DNA-PK and ATM will have a role in potentiating the effects of IR in the treatment of diseases such as breast cancer and that phosphorylation of H2AX could provide a useful biomarker to assess pharmacodynamic effects of this class of compound in vivo.

Acknowledgement

This work was supported by the Breast Cancer Campaign (2002/343).

Appendix A. Supplementary data

Supplementary data associated with this article can be found, in the online version, at doi:10.1016/j.bcp.2005.09.029.

REFERENCES

[1] Violet JA, Harmer C. Breast cancer: improving outcome following adjuvant radiotherapy. Br J Radiol 2004; 77:811–20.
[2] Jackson SP. Sensing and repairing DNA double-strand breaks. Carcinogenesis 2002;23:687–96.
[3] Rothkamm K, Kruger I, Thompson LH, Lobrich M. Pathways of DNA double-strand break repair during the mammalian cell cycle. Mol Cell Biol 2003;23:5706–15.
[4] Takata M, Sasaki MS, Sonoda E, Morrison C, Hashimoto M, Utsumi H, et al. Homologous recombination and non-homologous end-joining pathways of DNA double-strand break repair have overlapping roles in the maintenance of chromosomal integrity in vertebrate cells. EMBO J 1998;17:5497–508.
[5] Shiloh Y. ATM and related protein kinases: safeguarding genome integrity. Nat Rev Cancer 2003;3:155–68.
[6] Foray N, Priestley A, Alsbeih G, Badie C, Capulas EP, Arlett CF, et al. Hypersensitivity of ataxia telangiectasia fibroblasts to ionizing radiation is associated with a repair deficiency of DNA double-strand breaks. Int J Radiat Biol 1997;72:271–83.
[7] Kuhne M, Riballo E, Rief N, Rothkamm K, Jeggo PA, Lobrich M. A double-strand break repair defect in ATM-deficient cells contributes to radiosensitivity. Cancer Res 2004;64:500–8.
[8] Riballo E, Kuhne M, Rief N, Doherty A, Smith GC, Recio MJ, et al. A pathway of double-strand break rejoining dependent upon ATM, artemis, and proteins locating to γ-H2AX Foci. Mol Cell 2004;16:715–24.
[9] Chen G, Yuan SS, Liu W, Xu Y, Trujillo K, Song B, et al. Radiation-induced assembly of Rad51 and Rad52 recombination complex requires ATM and c-Abl. J Biol Chem 1999;274:12748–52.
[10] Morrison C, Sonoda E, Takao N, Shinohara A, Yamamoto K, Takeda S. The controlling role of ATM in homologous recombinational repair of DNA damage. EMBO J 2000;19:463–71.
[11] Griffin RJ, Fontana G, Golding BT, Guiard S, Hardcastle IR, Leahy JJ, et al. Selective benzopyranone and pyrimido[2,1-a]isoquinolin-4-one inhibitors of DNA-dependent protein kinase: synthesis, structure-activity studies, and radiosensitization of a human tumor cell line in vitro. J Med Chem 2005;48:569–85.
[12] Veuger SJ, Curtin NJ, Richardson CJ, Smith GC, Durkacz BW. Radiosensitization and DNA repair inhibition by the

combined use of novel inhibitors of DNA-dependent protein kinase and poly(ADP-ribose) polymerase-1. Cancer Res 2003;63:6008–15.
[13] Hickson I, Zhao Y, Richardson CJ, Green SJ, Martin NMB, Orr AI, et al. Identification and characterization of a novel and specific inhibitor of the ataxia-telangiectasia-mutated kinase ATM. Cancer Res 2004;64:9152–9.
[14] Izzard RA, Jackson SP, Smith GC. Competitive and non-competitive inhibition of the DNA-dependent protein kinase. Cancer Res 1999;59:2581–6.
[15] Rosenzweig KE, Youmell MB, Palayoor ST, Price BD. Radiosensitization of human tumor cells by the phosphatidylinositol 3-kinase inhibitors wortmannin and LY294002 correlates with inhibition of DNA-dependent protein kinase and prolonged G2-M delay. Clin Cancer Res 1997;3:1149–56.
[16] Boulton S, Kyle S, Durkacz BW. Mechanisms of enhancement of cytotoxicity in etoposide and ionising radiation-treated cells by the protein kinase inhibitor wortmannin. Eur J Cancer 2000;36:535–41.
[17] Vlahos CJ, Matter WF, Hui KY, Brown RF. A specific inhibitor of phosphatidylinositol 3-kinase, 2-(4-morpholinyl)-8-phenyl-4H-1-benzopyran-4-one (LY294002). J Biol Chem 1994;269:5241–8.
[18] Leahy JJ, Golding BT, Griffin RJ, Hardcastle IR, Richardson C, Rigoreau L, et al. Identification of a highly potent and selective DNA-dependent protein kinase (DNA-PK) inhibitor (NU7441) by screening of chromenone libraries. Bioorg Med Chem Lett 2004;14:6083–7.
[19] Bakkenist CJ, Kastan MB. DNA damage activates ATM through intermolecular autophosphorylation and dimer dissociation. Nature 2003;421:499–506.
[20] Banin S, Moyal L, Shieh SY, Taya Y, Anderson CW, Chessa L, et al. Enhanced phosphorylation of p53 by ATM in response to DNA damage. Science 1998;281:1674–7.
[21] Stiff T, O'Driscoll M, Rief N, Iwabuchi K, Lobrich M, Jeggo PA. ATM and DNA-PK function redundantly to phosphorylate H2AX after exposure to ionizing radiation. Cancer Res 2004;64:2390–6.
[22] Wang H, Wang M, Wang H, Bocker W, Iliakis G. Complex H2AX phosphorylation patterns by multiple kinases including ATM and DNA-PK in human cells exposed to ionizing radiation and treated with kinase inhibitors. J Cell Physiol 2005;202:492–502.
[23] Rogakou EP, Boon C, Redon C, Bonner WM. Megabase chromatin domains involved in DNA double-strand breaks in vivo. J Cell Biol 1999;146:905–16.
[24] MacPhail SH, Banath JP, Yu TY, Chu EH, Lambur H, Olive PL. Expression of phosphorylated histone H2AX in cultured cell lines following exposure to X-rays. Int J Radiat Biol 2003;79:351–8.
[25] Rothkamm K, Lobrich M. Evidence for a lack of DNA double-strand break repair in human cells exposed to very low X-ray doses. Proc Natl Acad Sci USA 2003;100:5057–62.
[26] Banath JP, Olive PL. Expression of phosphorylated histone H2AX as a surrogate of cell killing by drugs that create DNA double-strand breaks. Cancer Res 2003;63:4347–50.
[27] Reddy YV, Ding Q, Lees-Miller SP, Meek K, Ramsden DA. Nonhomologous end-joining requires that the DNA-PK complex undergo an autophosphorylation-dependent rearrangement at DNA ends. J Biol Chem 2004.
[28] Allen C, Halbrook J, Nickoloff JA. Interactive competition between homologous recombination and non-homologous end joining. Mol Cancer Res 2003;1:913–20.
[29] Ding Q, Reddy YV, Wang W, Woods T, Douglas P, Ramsden DA, et al. Autophosphorylation of the catalytic subunit of the DNA-dependent protein kinase is required for efficient end processing during DNA double-strand break repair. Mol Cell Biol 2003;23:5836–48.
[30] Burma S, Chen BP, Murphy M, Kurimasa A, Chen DJ. ATM phosphorylates histone H2AX in response to DNA double-strand breaks. J Biol Chem 2001;276:42462–7.
[31] Ward IM, Chen J. Histone H2AX is phosphorylated in an ATR-dependent manner in response to replicational stress. J Biol Chem 2001;276:47759–62.
[32] Zou L, Elledge SJ. Sensing DNA damage through ATRIP recognition of RPA-ssDNA complexes. Science 2003;300:1542–8.